FTIR Study of the Thermal Denaturation of α-Actinin in Its Lipid-Free and Dioleoylphosphatidylglycerol-Bound States and the Central and N-Terminal Domains of α-Actinin in D_2O[†]

Xing Han,* Guohong Li, Gang Li, and Kechun Lin

Department of Biophysics, Beijing Medical University, Beijing 100083, P. R. China

Received January 7, 1998; Revised Manuscript Received April 23, 1998

ABSTRACT: Fourier transform infrared (FTIR) spectroscopy has been carried out to investigate the thermal denaturation of α-actinin and its complexes with dioleoylphosphatidylglycerol (DOPG) vesicles. The amide I regions in the deconvolved spectra of α-actinin in the lipid-free and DOPG-bound states are both consistent with predominantly α-helical secondary structure below the denaturation temperatures. Studies of the temperature dependence of the spectra revealed that for α-actinin alone the secondary structure was unaltered up to 40 °C. But, in the presence of DOPG vesicles, the thermal stability of the secondary structure of α-actinin increased to 55 °C. The thermal denaturation mechanisms of the lipid-free and DOPG-bound states of α-actinin also vary. The secondary structure of the lipid-free α-actinin changed to be predominantly unordered upon heating to 65 °C and above. Whereas, the original α-helical structure in the DOPG-bound α-actinin retained even at 70 °C, the highest temperature we examined. Analysis of the reduction in amide II intensities, which is due to peptide H−D exchange upon heating α-actinin in D_2O, showed that partially unfolded states with increased solvent accessibility but substantial secondary structures could be observed from 35 to 40 °C only if DOPG vesicles were present. A so-called "protamine precipitation" method has been developed to purify the N-terminal domain of α-actinin by use of the fact that the central domain of α-actinin is negatively charged but the N-terminal domain is positively charged. Thermal denaturation of the central and N-terminal domains of α-actinin were then investigated with FTIR. The secondary structure of the N-terminal domain of α-actinin was found to be thermally sensitive below 35 °C, which is characterized as the increase of the α-helical structure at the expense of the random coil upon heating the N-terminal domain from 4 to 35 °C. The membrane-binding ability of the N-terminal domain of α-actinin was proposed in terms of the analysis of the local electrostatic properties of α-actinin and the assignment of the amide II bands in the FTIR spctra of α-actinin.

α-Actinin is an actin cross-linking and bundling protein that can be found both in muscle and nonmuscle cells (*1*). It is a homodimeric rod-shaped molecule (4−5 × 40−50 nm) with an antiparallel orientation of the subunits (*2*−*5*). Proteolysis cleaves α-actinin down to a 27−36 kDa N-terminal region, i.e., the actin binding domain, and a 55 kDa fragment, which is responsible for the formation of the homodimer (*6*−*9*). The C-terminal region of α-actinin contains two EF-hand, putative calcium-binding motifs (*10*).

Several kinds of membrane lipids including diacylglycerol (DG)[1] and palmitic acid (PA) (*11, 12*), phosphatidylinositol 4,5-bisphosphate (PIP_2) (*13, 14*), and negatively charged phospholipids (*15*−*17*) have been found to be able to interact with α-actinin in vivo and in vitro. It hints that α-actinin could play some important roles in the cytoskeleton−membrane interaction (for reviews, see refs *18, 19*). More recently, negatively charged phospholipids have been proved to be able to trigger the binding of α-actinin to lipid membranes (*17*), which might be the first step in the α-actinin−membrane interactions[2] and must be the critical step for linking actin filaments to the plasma membrane (*12, 19*) even though this linker-like ability of α-actinin has not yet been proved in vivo.[3] Therefore, an examination of the effects of negatively charged phospholipid on the conformation and conformational stability of α-actinin is of particular interest.

The conformational studies of α-actinin are very few so far, except that some circular dichroism (CD) results showed α-actinin was predominantly α-helical with little *β*-sheet in solution (*20, 21*). Cations and KCl have been stated to be able to induce the conformational changes of α-actinin (*21*).

[†] Supported by the National Natural Science Foundation of China.

* Author to whom correspondence should be addressed at Department of Molecular Physiology and Biological Physics, University of Virginia Health Sciences Center, Jordan Hall, Box 449, 1300 Jefferson Park Avenue, Charlottesville, VA 22908. Telephone: (804) 982-3281. Fax: (804) 982-1616. E-mail: xh3f@virginia.edu.

[1] Abbreviations: CD, circular dichroism; DG, diacylglycerol; DOPG, dioleoylphosphatidylglycerol; EDTA, ethylenediaminetetraacetic acid; FTIR, Fourier transform infrared spectroscopy; Hepes, 4-(2-hydroxyethyl)-1-piperazineethanesulfonic acid; PA, palmitic acid; PIP2, phosphatidylinositol 4,5-bisphosphate; PMSF, phenylmethanesulfonyl fluoride; SDS, sodium dodecyl sulfate.

[2] The other step could be the insertion process which seemingly needs the existence of DG in membrane as well as the negatively charged phospholipids (*16*) (for a discussion, see ref *17*).

[3] In vitro evidence indicates that α-actinin could link actin filaments to the lipid monolayer (*16*).

S0006-2960(98)00045-2 CCC: $15.00
Published on Web 07/09/1998

The purified central domain of α-actinin derived either from the proteolysis of α-actinin with α-chymotrypsin or from the bacterial expression comprises of four spectrin-like repeat sequences (*22*) and is high in α-helicity in solution (*8*, *23*). The structure of the isolated N-terminal domain of α-actinin has not been determined yet, although the globular N-terminal domain of α-actinin was purified with DEAE column after the proteolysis of α-actinin (*8*).

Our recent results showed that, besides the predominant α-helix, the *β*-sheet structure could also be resolved in the deconvolved FTIR spectra of α-actinin and its amount increased to some extent when α-actinin bound to dioleoylphosphatidylglycerol (DOPG) vesicles (*17*). To gain the structural information of α-actinin in solution and in association with DOPG vesicles in further detail, the thermal stability of α-actinin in the two different states has been investigated by FTIR upon heating from 4 to 70 °C with 5 °C increments in our present study. The secondary structures of the central and N-terminal domains of α-actinin as a function of temperature have also been studied by FTIR. The results were used to assign the conformational changed region in α-actinin when binding to DOPG vesicles. The N-terminal domain of α-actinin used in the FTIR study was purified by a so-called protamine precipitation method which has many advantages over the previous DEAE column method (*8*).

MATERIALS AND METHODS

Materials. Unless indicated, all the chemicals and reagents including DOPG, α-chymotrypsin (type II, from bovine pancreas), and protamine sulfate (Grade II, from salmon) were purchased from Sigma Chemical Co. DE-52 and Sepharose CL-6B, which were used in the purification of chicken gizzard α-actinin (*24*), were from Pharmacia Fine Chemicals. D_2O (99.8% pure) was from Beijing Chemical Factory. Water used in all experiments was doubly distilled.

Preparation of the Central Domain of α-Actinin. The central domain was prepared by the method of Kuroda et al. (*9*). Briefly, α-actinin was digested for 10 h in buffer A (30 mM NaCl, 10 mM Hepes, 0.2 mM EDTA, pH 7.4) with 1/100 (w/w) of α-chymotrypsin at 25 °C. Reaction was stopped by the addition of 1 vol of 1.0 mM PMSF. Precipitate obtained at 30% ammonium sulfate saturation was used as the isolated rod domain.

Preparation of Phospholipid Vesicles. Pure DOPG vesicles for the FTIR experiments were prepared in buffer B (30 mM NaCl, 10 mM Hepes, 0.2 mM EDTA in D_2O, pD 7.4). DOPG solution in chloroform/methanol (9:1) was dried briefly in a glass tube by a stream of nitrogen. After exposure to high vacuum for at least 2 h, the lipids were resuspended by vigorous vortexing in the buffer and then sonicated in a bath sonicator for 15 min at room temperature.

α-Chymotrypsin Digestion and Protamine Sulfate Precipitation. α-Actinin was digested from 0 to 60 min with α-chymotrypsin at an enzyme-to-substrate ratio of 1:75 (w/w) at 37 °C in buffer A. After the reaction was terminated by the addition of 1 vol of 1.0 mM PMSF solution, aliquots of protamine sulfate were added (protamine/α-actinin = 10:1, mol/mol) to trigger the protein aggregation. After being gently mixed for 30 s, suspensions were layered on top of 100 *μ*L of buffer A and centrifuged at 12000*g* for 3 min. Supernatants were carefully aspirated and collected. The pellets were washed twice with buffer A, and then they were dissolved in 10 *μ*L of buffer A and 10 *μ*L of SDS-sample buffer (10% w/v SDS, 20% v/v glycerol, 10% v/v 2-mercaptoethanol, and 0.125 M Tris/HCl, pH 6.8). The collected supernatants were lyophilized and were also dissolved in 10 *μ*L of buffer A and 10 *μ*L of SDS-sample buffer.

SDS−Polyacrylamide Gel Electrophoresis. SDS−polyacrylamide gel electrophoresis was carried out according to Laemmli (*25*) with 3% stacking and 10% separating gel. Gels were fixed with 20% trichloroacetic acid, stained with 0.25% Coomassie Brilliant Blue G-250 in a 50% aqueous methanol solution containing 12.5% trichloroacetic acid, and then destained with 7% acetic acid.

Preparation of N-Terminal Domain of α-Actinin by Protamine Precipitation Method. α-Actinin was digested for 30 min with α-chymotrypsin at an enzyme-to-substrate ratio of 1:75 (w/w) at 37 °C in buffer A. The reaction was terminated by the addition of 1 vol of 1.0 mM PMSF solution. After the addition of protamine sulfate (protamine/α-actinin = 10:1, mol/mol), the suspension was centrifuged at 12000*g* for 3 min. The supernatant which was rich in the N-terminal domain of α-actinin was collected and dialyzed extensively to remove any excess protamine sulfate.

FTIR Spectroscopy. Lyophilized α-actinin and its central and N-terminal domains in 30 mM NaCl, 0.2 mM EDTA, and 10 mM Hepes (pH 7.4) were dissolved in D_2O at 15 mg/mL. The proteins were incubated at 4 °C overnight to maximize H−D exchange. To study infrared amide bands of the proteins in the presence of lipids, small sonicated vesicles were mixed at desired proportion with the protein solution in buffer B to achieve the final protein concentration of 15 mg/mL. The sample was assembled between two calcium fluoride windows separated by a 25-*μ*m-thick Teflon spacer. The cell temperature controller was programmed to increase the temperature by 5 °C every 25 min. After a 15 min interval at each temperature setting to allow for thermal equilibration, the IR spectrum of the sample was collected. Infrared spectra were recorded with a Bio-Rad FTS 165 FT-IR spectroscope equipped with a DTGS detector. Each spectrum was obtained by collecting 400 interferograms with a nominal resolution of 4 cm^{-1}, and then was Fourier transformed using a triangular apodization function. Spectra of the buffer were recorded under identical conditions. The criterion used for subtracting buffers was the removal of the band near 2125 cm^{-1} and a flat baseline between 1770 and 2100 cm^{-1}. Fourier self-deconvolution of the subtracted spectra was carried out using a Bessel apodization function, a Lorentzian shape with a resolution enhancement parameter, *K*, of 2.4 and a full width at half-height of 13 cm^{-1}.

RESULTS

FTIR Studies of α-Actinin in D_2O Solution. Figure 1 shows the deconvolved spectra of α-actinin in D_2O in the 1800−1500 cm^{-1} region as a function of temperature from 4 to 70 °C.

Below 35 °C, the maximum absorption at 1649 cm^{-1} in the amide I region (1600−1700 cm^{-1}) of α-actinin is generally assigned to the α-helix. *β*-Sheet structure gives rise to the shoulder at 1633 cm^{-1}. On further increasing the temperature, α-actinin retains its secondary structure up

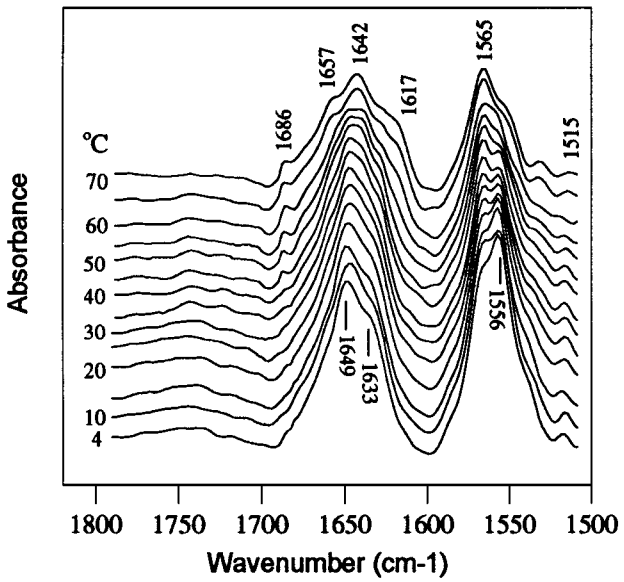

FIGURE 1: FTIR spectra of α-actinin in D_2O in the 1800−1500 cm^{-1} region as a function of temperature from 4 to 70 °C. Spectra were Fourier self-deconvolved with a resolution enhancement parameter of 2.4 and a full width at half-height of 13 cm^{-1}. Protein concentration was approximately 15 mg/mL.

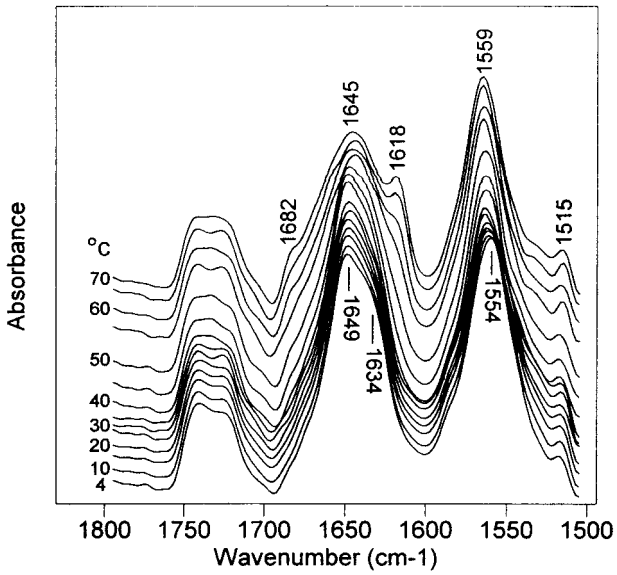

FIGURE 2: Deconvolved FTIR spectra of α-actinin in the presence of DOPG vesicles (lipid/protein = 600, mol/mol) in the 1800−1500 cm^{-1} region as a function of temperature from 4 to 70 °C.

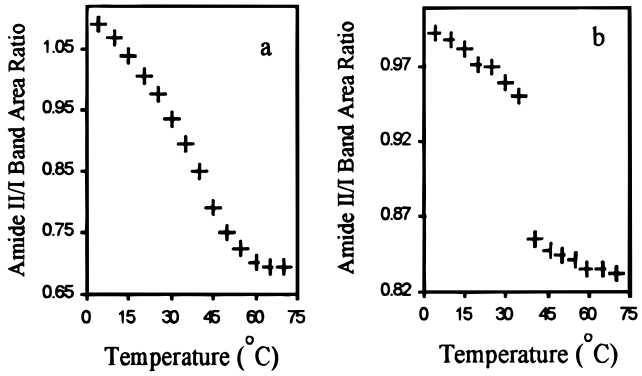

FIGURE 3: H−D exchange measurements by monitoring the deduction of the amide II/amide I area ratio as a function of temperture. α-Actinin was measured (a) in D_2O and (b) in the presence of DOPG vesicles (lipid/protein = 600, mol/mol).

to 40 °C. But there is an onset of an intermolecular hydrogen-bonded extended structure at 45 °C since a band at 1686 cm^{-1} was apparent at this temperature. This band is the result of the protein denaturation (*26*−*28*). A sudden increase in the intensity at 1641 cm^{-1} occurs at 50 °C, which can be interpreted in terms of an increase of the random coil structure. The denaturation of α-actinin appears to be complete at 65 °C since the aggregation bands (1686 and 1617 cm^{-1}) reached maximum intensity and the secondary structure of α-actinin is predominantly unordered at this temperature, which gives rise to the band at 1642 cm^{-1}. The appearance of the band at 1657 cm^{-1} at 65 °C indicates that a little amount of another type of α-helix which is characterized as higher amide I frequency (*29*−*31*) formed in α-actinin after its total denaturation.

In Figure 1, the band around 1515 cm^{-1} is pronouncedly present in all spectra and is assigned to tyrosine side chain absorption (*32*, *33*), which remains rather constant during heating. However, the intensities of two split peaks at 1556 and 1565 cm^{-1} in the amide II region (1600−1520 cm^{-1}) decrease gradually as a result of the H−D exchange. Since the amide I intensity was rather constant during heating, it was used as an internal standard in Figure 3. For each spectrum, the amide II area was then divided by the amide I area to take into account changes in the total intensity during the deuteration process. It was shown in Figure 3a that the amide II:amide I ratio exhibits a gradual decline over the entire temperature range.

FTIR Studies of α-Actinin in the Presence of DOPG Vesicles. Figure 2 shows the deconvolved spectra obtained from α-actinin in the presence of DOPG vesicles in the 1800−1500 cm^{-1} region as a function of temperature from 4 to 70 °C.

The lipid carbonyl stretching mode is responsible for the absorption between 1770 and 1710 cm^{-1}. Below 50 °C, the maximum absorption in the amide I region is at 1649 cm^{-1}, which indicates the predominant α-helical structure in α-actinin. The β-sheet structure gives rise to the band at 1634 cm^{-1}. The denaturation of DOPG-bound α-actinin occurs at 60 °C. This is characterized as the appearance of the bands at 1618 and 1682 cm^{-1} which indicates the formation of intermolecular hydrogen-bonded extended structure (*26*−*28*, *34*). Upon heating from 50 to 55 °C, there is a shift of the peak from 1649 cm^{-1} to around 1645 cm^{-1}. The peak around 1645 cm^{-1} was still assigned to the original α-helical structure by considering the facts that enhanced H−D exchange on heating could shift the α-helical absorption at 1649 to ∼1645 cm^{-1} (29, *35*−*38*), the temperature range, 50−55 °C, is lower than the denaturation temperature of DOPG-bound α-actinin (60 °C), and the new type of α-helical structure (∼1657 cm^{-1}) and the unordered structure (∼1642 cm^{-1}) did not appear even upon heating to 70 °C (see Figure 1; for further explanation, see Discussion).

The absorption of the DOPG-bound α-actinin in the amide II region does not split into two peaks as its lipid-free state, but shows only one major peak around 1554−1559 cm^{-1} (Figure 2, also see ref *17*). Figure 3b shows the H−D exchange of α-actinin in the presence of DOPG vesicles, which was represented by the ratio of integrated amide II intensity to amide I intensity, as a function of temperature.

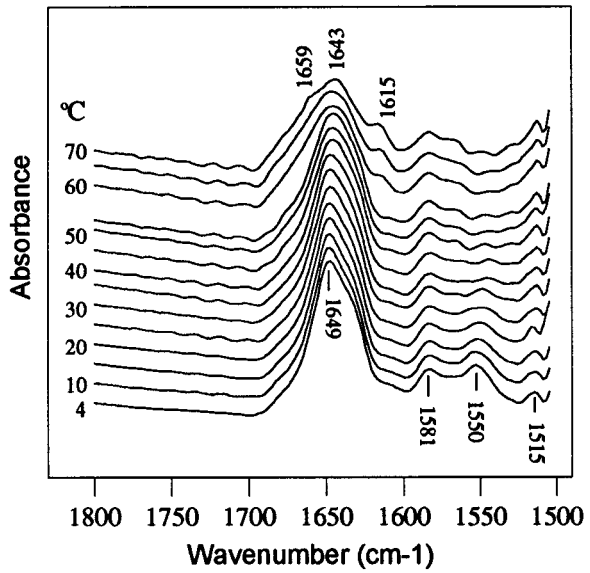

FIGURE 4: Deconvolved FTIR spectra of the central domain of α-actinin in D_2O in the 1800−1500 cm^{-1} region as a function of temperature from 4 to 70 °C. Protein concentration was approximately 15 mg/mL.

Table 1: Comparison of the Amide II Bands in the FTIR Spectra of α-Actinin and its N-Terminal and Central Domains

	1565 cm^{-1}	1556 cm^{-1}	1550 cm^{-1}
α-actinin[a]	+	+	
N-terminal domain[b]	+	+	
central domain[c]			+

[a] In D_2O, see Figure 1. [b] Precisely, the bands for the N-terminal domain of α-actinin are 1554 and 1566 cm^{-1}, see Figure 5. [c] See Figure 4.

Below 35 °C, the intensity ratio decreases gradually, which means the H−D exchange increased gradually. But there is an abrupt loss of the remaining intensity ratio upon heating from 35 to 40 °C, which indicates the loosening of the tertiary structure and hence the increased solvent penetration and H−D exchange (*29, 33*).

FTIR Studies of the Central Domain of α-Actinin in D_2O Solution. Figure 4 shows the deconvolved spectra of the central domain of α-actinin in the region of 1800−1500 cm^{-1} as a function of temperature from 4 to 70 °C. Below 55 °C, The central domain is predominantly α-helical, which gives rise to the major band at 1649 cm^{-1} in the amide I region. The intermolecular hydrogen-bounded structure of the central domain, which gives rise to the band at 1615 cm^{-1} in Figure 4, formed at 60 °C. This is in good agreement with the results of Flood and co-workers. They found that the denaturation temperature of the central domain of α-actinin was 55−60 °C (*39*). After the entire denaturation of the central domain at 70 °C, the secondary structure of the protein changed to be unordered which was characterized as the shift of the major absorption from 1649 to 1643 cm^{-1}. Similarly, the appearance of the band at 1659 cm^{-1} at 70 °C indicates that another type of α-helix formed (*29*−*31*).

The absorption bands of the central domain in the 1600−1500 cm^{-1} region is distinguishable from that of its parental protein, α-actinin (see Figure 4 vs Figure 1 and Table 1). In Figure 4, a band near 1581 cm^{-1} arises from the carboxylate group (*32, 33, 36, 40*), and the band at 1515 cm^{-1} is assigned

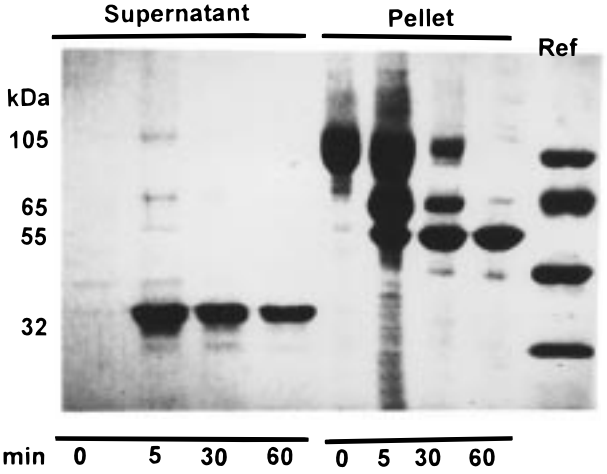

FIGURE 5: Identification of the protamine-associate fragment of α-actinin. (Methods) Aliquots of α-actinin were digested with α-chymotrypsin from 0 to 60 min at 37 °C separately. After the addition of protamine (protamine/α-actinin = 10:1, mol/mol), the suspensions were centrifuged at 12000*g* for 3 min. Fragments in supernatants and pellets were analyzed with SDS−PAGE (for details, see Materials and Methods). Refs., molecular weight standards: carbonic anhydrase (M_r = 29 kDa), actin (45 kDa), bovine serum albumin (66 kDa), and phosphorytase b (97.4 kDa).

to the tyrosine side chain (*32, 33*). Both bands retain their intensity during heating. The small band around 1550 cm^{-1} in the amide II region is due to the large degree of H−D exchange that has occurred and is obviously not related to the bands of α-actinin at 1556 and 1565 cm^{-1} in the amide II region (Figure 1). The amide II band of the central domain almost disappeared after heating to high temperature which indicates the total H−D exchange.

Purification of the N-Terminal Domain of α-Actinin by the Protamine-Precipitation Method. Protamine, a basic polypeptide (MW, 4000 to ∼5000) isolated from the condensed chromatin of salmon sperm, consists of about 80% arginine residues (*41*). It has been found that many acidic proteins, such as *Ah* receptor (*42*), androgen receptor (*43*), oestradiol receptor (*43*), and oestradiol-17 β protein (*44*), can form insoluble complexes with protamine in solution and even the acidic phospholipid vesicles can be quantitatively precipitated by protamine by the use of electrostatic interaction between them (*45, 46*).

Smooth muscle α-actinin is an acidic protein with a p*I* of 6.0 (*47*). The ability of α-actinin and its fragments to form the insoluble complexes with protamine were examined by us. Aliquots of α-actinin were first digested by α-chymotrypsin as a function of time. The products were then coprecipitated with protamine by low-speed centrifugation from the bulk solution. The supernatants and pellets were examined with SDS−PAGE separately. The results (Figure 5) showed that, at 0 min, most α-actinin could be coprecipitated with protamine (protamine/α-actinin = 10:1, mol/mol). Before and at 30 min, two fragments of 65- and 55 kDa were in pellets, but the 32 kDa fragment was left in supernatant. At 60 min, only the 55 kDa fragment could be in association with protamine. This result strongly suggests that the central domain (55 kDa), but not the N-terminal domain (32 kDa) of α-actinin, is responsible for the association of α-actinin with protamine (see Figure 7). The N-terminal domain is a basic segment of α-actinin with the p*I* ranging from about 7 to 8.85 (*7*), which could be the

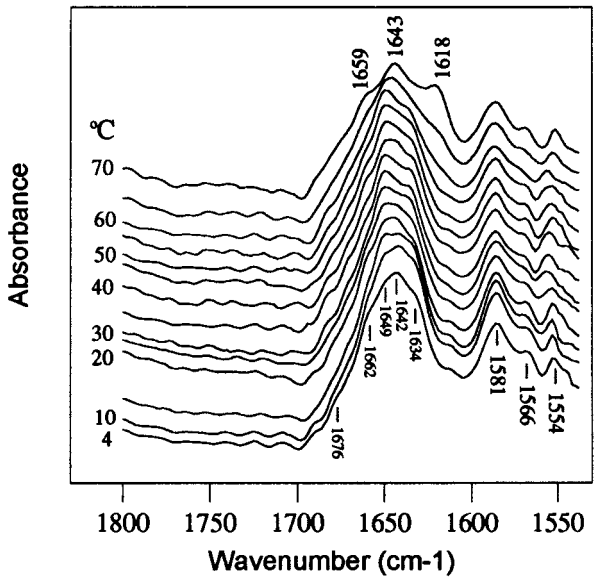

FIGURE 6: Deconvolved FTIR spectra of the N-terminal domain of α-actinin in D_2O in the 1800−1500 cm^{-1} region as a function of temperature from 4 to 70 °C.

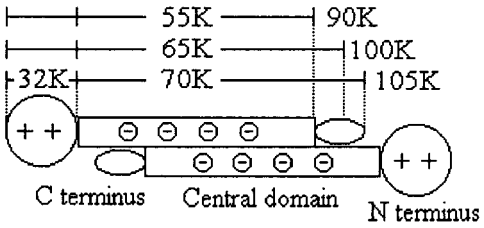

FIGURE 7: Cleavage and domain map of α-actinin, based on the results of Imamura et al. (*8*) and Han et al. (*17*). The N-terminal domain is positively charged (*7*) but the central domain is negatively charged (this paper).

reason that the N-terminus is not able to associate with the basic protamine.

An easy and rapid method, therefore, has been developed to isolate and purify the N-terminal domain of α-actinin by precipitation of the central domain with protamine from the mixture of the two fragments obtained by the chymotryptic digestion of α-actinin (for details, see Materials and Methods). The excess protamine can be removed by dialysis, which was examined by SDS−PAGE (data not shown). And the N-terminal domain purified with this method is able to bind to F-actin, which was examined by coprecipitation of their complex with centrifugation for 1 h at 100000*g* in a buffer containing 30 mM KCl, 3 mM $MgCl_2$, 1 mM EGTA, 0.2 mM ATP, 15 mM 2-mercaptoethanol, 1.5 mM NaN_3, and 40 mM Tris/HCl, pH 7.4 (data not shown). Besides the simplicity, the yield of this method is much higher than that of the DEAE column method (*8*) by our experience, which is critical for doing the FTIR measurements. Usually, 0.2 mg of the N-terminal domain can be obtained from 1 mg of α-actinin with this method.

FTIR Studies of the N-Terminal Domain of α*-Actinin in* D_2O *Solution*. Figure 6 shows the deconvolved spectra of the N-terminal domain in the amide I and amide II regions as a function of temperature from 4 to 70 °C. The N-terminal domain was purified by the protamine-precipitation method. It is found from the amide I band in the spectra that the secondary structure of the N-terminal domain of α-actinin is thermally sensitive from 4 to 35 °C. At 4 °C, at least five components can be resolved in the amide I band. The bands at 1676 and 1662 cm^{-1} arise from turns. The band at 1649 cm^{-1} is assigned to the α-helix. Random coil gives rise to the peak at 1642 cm^{-1}, which is in the highest intensity. The absorption at 1634 cm^{-1} is the lower frequency component of the β-sheet vibration. On heating from 4 to 35 °C, the absorption of the α-helix at 1649 cm^{-1} gradually increased at the expense of the absorption of the random coil structure at 1642 cm^{-1} and reached maximum around 35 °C. Above 30 °C but below 60 °C, the random coil (1642 cm^{-1}) structure could not be resolved any more in the amide I band, but the α-helical (1649 cm^{-1}) structure became predominant. The denaturation of the N-terminal domain occurred at 65 °C, which was characterized as the appearance of the absorption of the intermolecular β aggregation structure at 1618 cm^{-1} and the unordered structure at 1642 cm^{-1}. The absorption at 1659 cm^{-1} is still assigned to another type of α-helical structure (*29*−*31*).

In the 1600−1520 cm^{-1} region, the band at 1581 cm^{-1} arises from the carboxylate group (*33*, *36*, *40*). Two bands with low intensity at 1566 and 1554 cm^{-1} in the amide II region are apparent in Figure 6. The positions of the two bands are almost the same as those of the amide II bands of α-actinin in D_2O (see Table 1).

DISCUSSION

The Increased Thermal Stability of α*-Actinin When Binding to DOPG Vesicles*. We have investigated the structural nature of the thermal denaturation process for native α-actinin as well as its complexes with DOPG vesicles in the present study. It is known in the FTIR studies that interaction with membranes can lead to changes in protein stability (*48*−*50*); therefore, the changes that might occur on binding of α-actinin to DOPG vesicles are of particular interest.

In our study, the intermolecular hydrogen-bonded extended structure in proteins, which gives rise to the bands around 1686 or/and 1617 cm^{-1} in the FTIR spectra, was used as a sign of the protein denaturation. The feasibility of this method is based on the results of many earlier thermal denaturation studies of proteins with FTIR (*26*−*28*, *34*) and is reinforced by our observation that, in the spectra of the central domain of α-actinin, a band at 1615 cm^{-1} appeared at 60 °C (Figure 4) which is exactly the denaturation temperature of the central domain of α-actinin (*39*). Thus, we concluded that the denaturation of α-actinin in D_2O and α-actinin in the presence of DOPG vesicles took place at 45 °C (Figure 1) and 60 °C (Figure 2), respectively. This means that the structure of α-actinin has more thermal stability in its DOPG-bound state.

There is a common feature for α-actinin (Figure 1), its central domain (Figure 4), and N-terminal domain (Figure 6) that, when their denaturation reached completion or near-completion, a band around 1659 cm^{-1} appeared. This band arises from another type of α-helical structure which is different from the one that gives rise to the band at 1649 cm^{-1} (*29*−*31*). Besides, along with the appearance of the band at 1659 cm^{-1}, the original α-helical structure at 1649 cm^{-1} disappeared but the random coil structure around 1642 cm^{-1} showed up. This revealed the mechanism of the

denaturation of α-actinin; i.e., a small part of the original α-helical structure in α-actinin switched to a new type of α-helix but the other part changed to random coil structure after the denaturation of α-actinin. Comparably, when α-actinin bound to DOPG vesicles, both the bands at 1659 and 1642 cm^{-1} did not appear even upon heating to 70 °C (Figure 2). Therefore, we concluded that the original α-helix in DOPG-bound α-actinin retained even at such high temperature. The reason for the band shift from 1649 to 1645 cm^{-1} at 55 °C most probably is the enhanced deuteration of the amide carbonyl groups of α-helical domains in α-actinin.

H−D Exchange Measurements as a Function of Temperature. H−D exchange has long been recognized as a powerful method for the study of protein conformational dynamics. The rate and extent of H−D exchange in proteins may be obtained with FTIR by measuring the decrease in intensity of the amide II band of the protein (*28*, *33*, *49*, *51*). Much information on the structure, dynamics, and water accessibility of proteins in the native state and in association with lipid membranes came from the measurements of the H−D exchange kinetics with FTIR (*35*, *49*, *51*−*54*). Recently, the stable folding intermediates of some proteins have been observed with FTIR by the measurements of H−D exchange of proteins upon heating (*29*, *33*). The stable folding intermediates of these proteins were all characterized as an enhanced hydrogen exchange without concomitant secondary structure change and were interpreted as a partially unfolded state with intact secondary structure but collapsed or highly flexible tertiary structure (*33*).

We also measured the H−D exchange of α-actinin in the absence and in the presence of DOPG vesicles as a function of temperature (Figure 3). We found that the H−D exchange of α-actinin in D_2O increased gradually upon heating (Figure 3a). This could be the co-effects of the increased kinetic energy of the NH bonds and protein unfolding (*33*). We cannot know, in terms of Figure 3a, which kind of intermediate, i.e., kinetic or equilibrium intermediate, that α-actinin adopted from folding to unfolding in the absence of DOPG vesicles. But in the case of α-actinin in association with DOPG vesicles, there was an abrupt enhancement of H−D exchange between 35 and 40 °C (Figure 3b), which occurred about 20 °C ahead of the secondary structural denaturation (Figure 2). According to van Stokkum et al. (*33*), this should be attributed to the so-called partially unfolded state of α-actinin.

Thermally Sensitive Secondary Structure of the N-Terminal Domain of α-Actinin in the Native State. Upon heating from 4 to 35 °C, there is an apparent secondary structural change in the N-terminus, the actin binding domain of α-actinin. It is characterized as the transfer from random coil to α-helix (see Figure 6).

It is known that the binding behavior of α-actinin to actin is temperature dependent. The dissociation rate constant of α-actinin from F-actin increased concomitantly with the increase of temperature (*11*, *55*). α-Actinin binds along the entire length of the F-actin strand at low temperature (0 °C), whereas at higher temperature (37 °C), binding of α-actinin is restricted to one end, the Z-line end, of the F-actin strand (*56*, *57*). It has been proposed that the binding of α-actinin to F-actin is regulated by conformational changes of α-actinin related either to the changes of molecular axial ratio (*9*, *57*, *58*) or to partial unfolding of the protein (*57*). In our present study, it is found that the secondary structure of the actin binding domain of α-actinin, i.e., the N-terminal domain, is thermally sensitive from 4 to 35 °C. This might be a potential interpretation for the temperature-dependent behavior of α-actinin when binding to F-actin, although the direct relationship between them has not yet been built up.

Is the N-Terminal Domain Responsible for the Binding of α-Actinin to the Membranes Containing Negatively Charged Phospholipid? α-Actinin is an acidic protein with a p*I* of 6.0 (*47*). Previous results showed that Ca^{2+} was unable to influence the membrane-binding behavior of α-actinin (*17*). There would be a question that how the acidic protein binds to the acidic membrane through the electrostatic interaction.

The result of the protamine-precipitation experiment (Figure 5) indicates that the central domain of α-actinin is rich in negative charges, which led to the insoluble complex formation between α-actinin and the strongly basic peptide, protamine. It is already known that the N-terminal domain of α-actinin contains net positive charges (*7*). The local electrostatic properties of α-actinin, therefore, can be shown as in Figure 7.[4] This could be the answer of how α-actinin is able to bind to membranes containing negatively charged phospholipid through the electrostatic interaction. In other words, it hints the positively charged N-terminal domain of α-actinin could be responsible for the binding of α-actinin to the negatively charged membrane. It is well-known that electrostatic effects play an essential role in the protein−protein interactions (for a review, see ref *59*). Therefore, this local electrostatic property of α-actinin could also be very important in the actin/α-actinin interaction.

Another evidence which supports the assumption that the N-terminal domain is the membrane-binding domain of α-actinin comes from the FTIR results. It is shown in Table 1 that the positions of the amide II bands are the same for α-actinin (in D_2O) and its N-terminal domain. Both of them have absorption around 1565 and 1556 cm^{-1} (for the N-terminus, the bands are 1566 and 1554 cm^{-1}). But, for the central domain of α-actinin, its absorption in the amide II region is around 1550 cm^{-1}. It means that, in D_2O, the absorption of α-actinin in the amide II region is mainly attributed to its N-terminal domain. The contribution of the central domain of α-actinin to α-actinin amide II's absorption at 1550 cm^{-1} might be so small, because of the fast H−D exchange of the central domain, that it cannot be resolved in the spectrum.[5]

Based on the above assignment, conformationally changed domain of α-actinin induced by negatively charged phospholipid can be assigned to the N-terminus. In the presence of vesicles containing negatively charged phospholipid, the absorption characteristic of α-actinin in the amide II region changed greatly (*17*) (see Figure 2). Only one major band around 1554 (at 4 °C) showed (Figure 2) instead of two bands at 1556 and 1565 cm^{-1} in the absence of negatively charged phospholipid (*17*) (see Figure 1). It indicates the secondary structure of α-actinin changed when it bound to membranes containing negatively charged phospholipid (*17*), and this

[4] The C-terminal domain is ignored.

[5] We cannot exclude the contribution of the C-terminal domain of α-actinin to the amide II absorption of α-actinin so far. But we assume here that the main contribution is from the N-terminal domain.

change should occur in the N-terminal domain of α-actinin. We already knew that the folding−unfolding processes of α-actinin are different in the absence and in the presence of negatively charged phospholipid (see Figure 3 and the above text). The partially unfolded states could only be observed if DOPG vesicles were present. This conclusion comes from the measurements of the reduction in the amide II intensities upon heating. Because the amide II absorption of α-actinin in D_2O was mainly from its N-terminal domain, the observed partially unfolded states of α-actinin induced by DOPG should also occur in the N-terminal domain. The influence of negatively charged phospholipid on the structure and folding−unfolding process of the N-terminal domain strongly supports the conclusion that the N-terminal domain has a direct relationship with negatively charged phospholipid. It is therefore reasonable to presume that the N-terminal domain could be the membrane-binding domain of α-actinin.

We can see from Figures 1 and 2 that, at low temperatures, the intensities of the amide II bands of α-actinin are somewhat surprisingly high. For most proteins measured in D_2O with FTIR spectroscopy, the intensities of their amide II bands are usually very low due to H−D exchange resulting in the shift of this band toward lower frequency. This is the reason that the FTIR spectra of the central and N-terminal domains of α-actinin do not show strong absorption in the amide II region (Figures 4 and 6). The best interpretation for the strong absorption of α-actinin in the amide II region could be that the folding behaviors of the intact pretein and its fragments are different in D_2O. α-Actinin could be folded much more tightly than its fragments, which inhibits the penetration of D_2O molecules into the interior of α-actinin.

PIP_2, a special membrane lipid, was found to be able to dramatically increase the gelating activity of smooth muscle α-actinin (*13*). And most recently, the PIP_2 binding-site of α-actinin has just been identified as the amino acids 168−184 in its N-terminal domain (*14*). Hence, it would be very significant if PIP_2 could regulate the gelating activity of α-actinin in the plasm membrane plane to which α-actinin binds with its N-terminal domain.

REFERENCES

1. Baron, M. D., Davison, M. D., Jones, P., and Critchley, D. R. (1987) *Biochem. Soc. Trans. 15*, 796−798.
2. Podlubnaya, Z. A., Tskhovreova, L. A., Zaalisnvili, M. M., and Stefanenko, G. A. (1975) *J. Mol. Biol. 92*, 357−389.
3. Suzuki, A., Goll, D. E., Stromer, M. H., Singh, I., and Temple, J. (1976) *J. Biol. Chem. 251*, 6860−6870.
4. Wallraff, E., Schlecher, M., Modersitzki, M., Rieger, D., Isenberg, G., and Gerisch, G. (1986) *EMBO J. 5*, 61−67.
5. Meyer, R. K., and Aebi, U. (1990) *J. Cell Biol. 110*, 2013−2024.
6. Mimura, N., and Asano, A. (1986) *J. Biol. Chem. 261*, 10680−10687.
7. Mimura, N., and Asano, A. (1987) *J. Biol. Chem. 262*, 4717−4723.
8. Imamura, M., Endo, T., Kuroda, M., Tanaka, T., and Masaki, T. (1988) *J. Biol. Chem. 263*, 7800−7805.
9. Kuroda, M., Kohira, Y., and Sasaki, M. (1994) *Biochim. Biophys. Acta 1205*, 97−104.
10. Noegel, A., Witke, W., and Schleicher, M. (1987) *FEBS Lett. 221*, 391−396.
11. Meyer, R. K., Schindler, H., and Burger, M. M. (1982) *Proc. Natl. Acad. Sci. U.S.A. 79*, 4280−4284.
12. Burn, P., Rotman, A., Meyer, R. K., and Burger, M. M. (1985) *Nature 314*, 469−472.
13. Fukami, K., Furuhashi, K., Inagaki, M., Endo, T., Hatano, S., and Takenawa, T. (1992) *Nature 359*, 150−152.
14. Fukami, K., Sawada, N., Endo, T., and Takenawa, T. (1996) *J. Biol. Chem. 271*, 2646−2650.
15. Niggli, V., and Gimona, M. (1993) *Eur. J. Biochem. 213*, 1009−1015.
16. Fritz, M., Zimmermann, R. M., Bamann, M., and Gaub, H. E. (1993) *Biophys. J. 65*, 1878−1885.
17. Han, X., Li, G., Li, G., and Lin, K. (1997) *Biochemistry 36*, 10364−10371.
18. Niggli, V., and Burger, M. M. (1987) *J. Membr. Biol. 100*, 97−121.
19. Burn, P. (1988) *Trends Biochem. Sci. 13*, 79−83.
20. Blanchard, A., Ohanian, V., and Critchley, D. R. (1989) *J. Muscle Res. Cell Motil. 10*, 280−289.
21. Wenegieme, E. F., Babitch, J. A., and Naren, A. P. (1994) *Biochim. Biophys. Acta 1205*, 308−316.
22. Baron, M. D., Davison, M. D., Jones, P., and Critchley, D. R. (1987) *J. Biol. Chem. 262*, 17623−17629.
23. Gilmore, A. P., Parr, T., Patel, B., Gratzer, W. B., and Critchley, D. R. (1994) *J. Biochem. 225*, 235−242.
24. Feramisco, J. R., and Burridge, K. (1980) *J. Biol. Chem. 255*, 1194−1199.
25. Laemmli, U. K. (1970) *Nature 227*, 680−685.
26. Clark, A. H., Saunderson, D. H. P., and Suggett, A. (1981) *Int. J. Pept. Protein Res. 17*, 353−364.
27. Ismail, A. A., Mantsch, H. H., and Wong, P. T. T. (1992) *Biochim. Biophys. Acta 1121*, 183−188.
28. Jiang, H., Song, Z., Ling, M., Yang, S., and Du, Z. (1996) *Biochim. Biophys. Acta 1294*, 121−128.
29. Holzbaur, I. E., English, A. M., and Ismail, A. A. (1996) *Biochemistry 35*, 5488−5494.
30. Prestrelski, S. J., Byler, D. M., and Thompson, M. P. (1991) *Int. J. Pept. Protein Res. 37*, 508−512.
31. Tatulian, S. A., Biltonen, R. L., and Tamm, L. K. (1997) *J. Mol. Biol. 268*, 809−815.
32. Goormaghtigh, E., Cabiaux, V., and Ruysschaert, J.-M. (1994) in *Physicochemical Methods in the Study of Biomembranes* (Hildeson, H. J., and Ralston, G. B., Eds.) pp 329−361, Plenum Press, New York.
33. Van Stokkum, I. H. M., Linsdell, H., Hadden, J. M., Haris, P. I., Chapman, D., and Bloemendal, M. (1995) *Biochemistry 34*, 10508−10518.
34. Medrano, F. J., Gasset, M., Sopez-Zumel, C., Usobiaga, P., Garcia, J. L., and Menendez, M. (1996) *J. Biol. Chem. 271*, 29152−29161.
35. Zhang, Y.-P., Lewis, R. N. A. H., Henry, G. D., Sykes, B. D., Hodges, R. S., and McElhaney, R. N. (1995) *Biochemistry 34*, 2348−2361.
36. Chirgadze, Y. N., Brazhnikov, E. V., and Nevskaya, N. A. (1976) *J. Mol. Biol. 102*, 781−792.
37. Rabolt, J. F., Moore, W. H., and Krimm, S. (1977) *Macromolecules 10*, 1065−1074.
38. Dwivedi, A. M., and Krimm, S. (1984) *Biopolymers 23*, 923−943.
39. Flood, G., Rowe, A. J., Critchley, D. R., and Gratzer, W. B. (1997) *Eur. Biophys. J. 25*, 431−435.
40. Venyaminov, S. Yu., and Kalnin, N. N. (1990) *Biopolymers 30*, 1243−1257.
41. Richards, R. G., and Shaw, B. R. (1982) *Anal. Biochem. 121*, 69−82.
42. Denison, M. S., Fine, J., and Wilkinson, C. F. (1984) *Anal. Biochem. 142*, 28−36.
43. King, R. J. B., Gordon, J., and Steggles, A. W. (1969) *Biochem. J. 114*, 649−656.
44. Steggles, A. W., and King, R. J. B. (1970) *Biochem. J. 118*, 695−701.
45. Rosier, R. N., Gunter, T. E., Tucker, D. A., and Gunter, K. K. (1979) *Anal. Biochem. 96*, 384−390.
46. Gunter, K. K., Gunter, T. E., Jarkowski, A., and Rosier, R. N. (1982) *Anal. Biochem. 120*, 113−124.
47. Pollard, T. D., Tseng, P. C. H., Rimm, D. L., Bichell, D. P., Williams, R. C., Jr., Sinard, J., and Sato, M. (1986) *Cell Motil. Cytoskeleton 6*, 649−661.

48. Muga, A., Mantsch, H. H., and Surewicz, W. K. (1991) *Biochemistry 30*, 7219−7224.
49. Heimburg, T., and Marsh, D. (1993) *Biophys. J. 65*, 2408−2417.
50. Swamy, M. J., Heimbrug, T., and Marsh, D. (1996) *Biophys. J. 71*, 840−847.
51. Hadden, J. M., Bloemendal, M., Haris, P. I., Srai, S. K. S., and Chapman, D. (1994) *Biochim. Biophys. Acta 1205*, 59−67.
52. Jung, E. K. Y., Chin, J. J., and Jung, C. Y. (1986) *J. Biol. Chem. 261*, 9155−9160.
53. Vigneron, L., Ruysschaert, J.-M., and Goormaghtigh, E. (1995) *J. Biol. Chem. 270*, 17685−17696.
54. Raussens, V., Narayanaswami, V., Goormaghtigh, E., Ryan, R. O., and Ruysschaert, J.-M. (1996) *J. Biol. Chem. 271*, 23089−23095.
55. Sato, S. B., Schwarz, W. H., and Pollard, T. D. (1987) *Nature 325*, 828−830.
56. Robson, R. M., Goll, D. E., Arakawa, N., and Stromer, M. H. (1970) *Biochim. Biophys. Acta 200*, 297−318.
57. Goll, D. E., Suzuki, A., Temple, J., and Holmes, G. R. (1972) *J. Mol. Biol. 67*, 469−488.
58. Holmes, G. R., Goll, D. E., and Suzuki, A. (1971) *Biochim. Biophys. Acta 253*, 240−253.
59. Nakamura, H. (1996) *Q. Rev. Biophys. 29*, 1−90.

BI9800451